Tropical Cold Point Tropopause Characteristics Derived from ECMWF Reanalyses and Soundings

XUELONG ZHOU, MARVIN A. GELLER, AND MINGHUA ZHANG

Institute for Terrestrial and Planetary Atmospheres, State University of New York at Stony Brook, Stony Brook, New York

(Manuscript received 18 January 2000, in final form 31 July 2000)

ABSTRACT

Tropical cold point tropopause (CPT) characteristics have been calculated using ECMWF reanalyses and high resolution radiosonde soundings obtained in TOGA COARE as well as operational sounding data. It is found that ECMWF reanalyses are suitable for investigating the morphology of the tropical CPT and the variabilities of the tropopause over the entire Tropics, despite an almost constant one-side warm bias. The daily locations of the tropical coldest CPT are clustered over the western Pacific warm pool region in January and spread out longitudinally as the year progresses. During the Indian summer monsoon, the locations of the coldest CPT are deflected northward.

The influences of the quasi-biennial oscillation (QBO) and the El Niño–Southern Oscillation (ENSO) on the tropical CPT have been separated using bivariate regression. The stratospheric zonal wind shear at 50 mb leads the variation in the tropical CPT temperatures by about 6 months. The QBO signature in the tropical CPT is mainly zonally symmetric and is consistent with the downward propagating tropical stratospheric QBO meridional circulation. CPT temperatures and the sea surface temperature anomalies (SSTAs) in the Niño-3.4 region are simultaneously correlated. The fingerprints of the ENSO in the CPT show east–west dipole and north–south dumbbell features, which can be explained by changes of convection during ENSO events. The interference between the QBO and ENSO effects on the tropical CPT, and the effect of the quasi-biennial oscillations in SSTA are discussed. The low-frequency variabilities of the CPT related to the QBO and ENSO can be a cause of the observed interannual variability of stratospheric water vapor because they affect the entry values of the water vapor mixing ratio across the tropical CPT to the stratosphere.

1. Introduction

It is generally acknowledged that the residual circulation, with upwelling in the Tropics and downwelling in polar regions, dominates Stratosphere Troposphere Exchange (STE), and that the cold tropical tropopause temperatures are crucial to stratospheric dryness (Holton et al. 1995). However, many aspects of the coupling between the tropical troposphere and the tropical stratosphere are still not clear.

Newell and Gould-Stewart (1981) noted that tropopause temperatures are cold enough to account for observed water vapor mixing ratios in the lower stratosphere only during certain months and at certain locations. They showed that sufficiently cold temperatures were frequently found over the maritime continent warm pool region in January and were also found, though less frequently, over the Indian summer monsoon region during July. They suggested that tropospheric air entered the stratosphere mostly at these preferred times and locations. This is the ''stratospheric fountain'' hypothesis. Dessler (1998) re-examined the stratospheric fountain hypothesis by comparing estimates of the entry value of water vapor entering the stratosphere derived from midlatitude stratospheric observations (Abbas et al. 1996; Dessler et al. 1994; Hanson and Robinson 1989; Jones et al. 1986; Remsberg et al. 1996), to annually and zonally averaged estimates of the minimum saturation mixing ratio at the tropical tropopause. Based on his calculations for the period 1994–97, he concluded that the stratospheric fountain hypothesis is not necessary, implying that tropospheric air can enter the stratosphere at any longitude in the Tropics rather than at preferred regions at preferred times. Zhou et al. (2001), however, found a cooling trend of tropical tropopause temperatures after examining an extended version of the same dataset used by Dessler (1998). Dessler (1998) happened to have selected the coldest years that existed during the period dating back to 1973. This cooling trend in the tropical cold point tropopause (CPT) indicates that the stratospheric fountain hypothesis is still necessary.

Corresponding author address: Dr. Marvin Geller, Marine Science Research Center, State University of New York at Stony Brook, Stony Brook, NY 11794-5000.
E-mail: mgeller@notes.cc.sunysb.edu

The purpose of the present study is to investigate the morphology and variability of the tropical CPT so as to provide some bases for further study of these issues. Features of the tropical tropopause have been reported in several earlier studies (e.g., Reid and Gage 1981, 1985, 1996; Frederick and Douglass 1983; Gage and Reid 1987). The present study differs from these previous works in three aspects. First, we investigate the CPT rather than the lapse rate tropopause. There are a few different definitions of the tropopause, among which the traditional World Meteorological Society (WMO) lapse rate tropopause has the least physical meaning in the Tropics, and the CPT is most relevant to STE in the Tropics (Highwood and Hoskins 1998). Second, previous studies have been limited to sparse tropical sounding stations. In this paper, we will show features of the tropical CPT over the entire Tropics. Finally, we will show several features of the variability of the tropical CPT that have not been reported before. This includes the seasonal cycle of the stratospheric fountain,[1] and the low-frequency variabilities of the tropical tropopause that are related to the stratospheric quasi-biennial oscillation (QBO) and tropospheric El Niño–Southern Oscillation (ENSO).

The paper is organized as follows. In section 2, we discuss the reliability of using the European Centre for Medium-Range Weather Forecasts (ECMWF) reanalyses to investigate tropical tropopause variability, and show the horizontal features of the tropical CPT, particularly the stratospheric fountain. The variabilities of the tropical CPT related to the QBO and ENSO are investigated in section 3. Section 4 contains further discussions on related topics, and the last section summarizes the paper.

[1] Stratospheric fountain is a historical term that was proposed according to analysis of the temperature field (Newell and Gould-Stewart 1981) and refers to the region where the tropical tropopause is cold enough to dehydrate air parcels entering the stratosphere across the tropopause to match the observed low concentration of stratospheric water vapor. Sherwood (1999) and Gettelman et al. (2000) recently found that the western Pacific might be a ''stratospheric drain'' instead of a ''stratospheric fountain'' according to their analyses of the wind field. A few wind-profiling Doppler radar measurements over Pohnpei suggested that cooling at the top of the anvils will result in downward motion above the anvils (Gage et al. 1991). However, convection may frequently overshoot the tropical tropopause (Danielsen 1993; Holton et al. 1995), and a large-scale ascent in the upper troposphere to the lower stratosphere is expected due to diabatic heating in the middle troposphere even if convection does not overshoot the tropopause (Highwood and Hoskins 1998). It is difficult to explain the observed low concentration of stratospheric water vapor unless the western Pacific determines the dehydration of air entering the stratosphere regardless where and when the entry takes place (this paper and Zhou et al. 2001). The role of tropical convection in stratosphere–troposphere exchange is not well known. Further investigations are needed to classify whether the western Pacific is a fountain or a drain to the stratosphere, which are important but beyond the scope of this paper. The term stratospheric fountain is used in the remainder of the text simply for us to conveniently compare our analyses of the CPT with previous results.

Since the principal purpose of our tropopause calculations is to infer the thermal effect of the tropical tropopause in determining stratospheric dryness, the ''tropopause'' in this paper was simply defined as the position where the minimum Saturation Mixing Ratio (SMR) of water vapor with respect to ice is found in the vertical profile.[2] The CPT is usually defined as the position of the minimum temperature in the vertical temperature profile (Highwood and Hoskins 1998). We have calculated the tropical CPT following these two definitions and have found the difference between the minimum-temperature tropopause and the minimum-SMR tropopause to be small as shown in Fig. 1, so that we call the minimum-SMR tropopause the CPT, thus avoiding a new term.

2. Data intercomparison and CPT features

Three principal datasets are utilized in this study: ECMWF reanalyses (Gibson et al. 1997), high resolution Tropical Oceans and Global Atmosphere Coupled Ocean–Atmosphere Response Experiment (TOGA COARE) balloon soundings, and operational radiosonde soundings. The National Centers for Environmental Prediction (NCEP) reanalyses have been used for a brief comparison only. Stratospheric zonal wind shear at 50 mb over Singapore,[3] and SST anomalies (SSTAs) in the Niño-3.4 region (5°N–5°S, 120°–170°W) are used as indices for the stratospheric QBO and tropospheric ENSO, respectively.

We used the gridded (2.5° × 2.5°) version of ECMWF reanalyses that are available at 17 standard pressure levels 4 times per day for 1979–93. The ECMWF reanalyses have global coverage, but have coarse vertical spacing near the tropopause (the ECMWF reanalyses pressure levels near the tropical tropopause are 200, 150, 100, 70, and 50 mb). The properties of the tropical CPT (pressure, temperature, height, SMR) in ECMWF reanalyses have to be interpolated. Also, of course, the ECMWF reanalyses are a model-data mixture rather than pure observational data. Operational rawinsonde data from 1973 to 1998 (26 yr) are also used. Operational sounding profiles usually have about 5–20 records in the range of 70 to 200 mb, making interpolated tropopause properties more accurate. We used a cubic spline (in log pressure) interpolation to determine the cold-point tropopause from the ECMWF reanalyses and the operational sounding data. The TOGA COARE soundings are available for 1 yr (from July 1992 to June 1993) for a few stations such as Kapingamarangi (1.07°N, 154.80°E), and are available for about 4 months (November 1992–February 1993) for most of the par-

[2] Dessler (1998) also used this to avoid the complexity of the tropopause definition.

[3] Stratospheric wind data were obtained from Barbara Naujokat, Freie Universitaet Berlin.

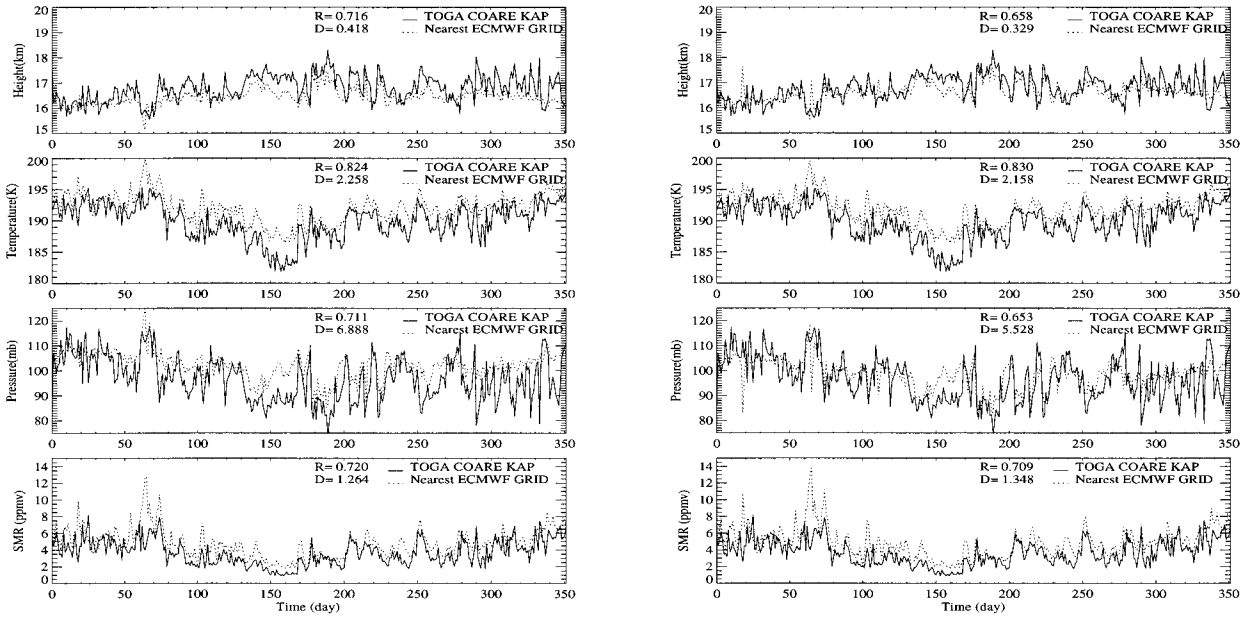

(a) Minimum-SMR CPT (b) Minimum-Temperature CPT

FIG. 1. CPT at KAP from TOGA COARE soundings and ECMWF reanalyses.

ticipating stations. The balloons were released 4 times per day and sounding data were recorded every 10 s. The vertical resolution of the TOGA COARE soundings is so fine that we can obtain the CPT directly from the observations. The advantages of each dataset will be exploited for different purposes in this study.

For the ECMWF reanalyses, we calculated the CPT properties 4 times per day and averaged them to obtain the daily mean. These daily means are saved for further investigation. Figure 1 shows the comparison between the daily mean CPT properties at Kapingamarangi and those at the nearest ECMWF grid point.[4] TOGA COARE sounding data at Kapingamarangi were available from 11 July 1992 to 29 June 1993. The few days when all four TOGA COARE soundings missed the CPT are deleted, so the days in Fig. 1 are not consecutive. There is excellent tracking of the cold-point temperature ($R = 0.824$) and somewhat lesser tracking of the cold-point pressure ($R = 0.711$) between the Kapingamarangi sounding and that determined by applying the spline fitting to the nearest ECMWF grid point. The SMRs at the ECMWF grid point nearest to Kapingamarangi and those from the sounding at Kapingamarangi compare very well ($R = 0.720$). It does appear that the ECMWF reanalyses overestimate the cold point temperatures by about 2 K (on the average) as well as overestimates the pressures a bit (about 7 mb), and this results in an overestimate of the cold-point saturation water vapor mixing ratio by about 1.3 ppmv. We have compared ECMWF-based calculations with all available TOGA COARE and operational soundings, and found that the ECMWF reanalyses track the CPT very well even at subtropical sounding stations (e.g., Hong Kong). ECMWF reanalyses systematically have a one-side warm bias compared with soundings at all sounding stations except on a few days. By comparing the ECMWF-based calculations with the CPT properties from TOGA COARE soundings and operational soundings, we have found that the smallest warm bias is over the western Pacific (about 2 K), and the largest warm bias is over tropical Africa (about 2.6 K).

In order to see if the ECMWF reanalyses can be used to study low-frequency variability of the CPT, it is necessary to compare the results from ECMWF reanalyses with the results from soundings over a relatively long period. We have compared regional monthly anomalies of the CPT properties from ECMWF based calculations and those from operational soundings. We first divided the Tropics (10°S–10°N) into 7 regions arbitrarily according to longitude (0°–45°E, 45°–90°E, 90°–150°E, 150°–205°E, 205°–270°E, 270°–320°E, and 320°–360°E, called R1, R2, R3, R4, R5, R6, and R7, respectively). We have constructed the monthly mean CPT temperature, pressure, and SMR based on the operational soundings for each region (except R5 where there are not enough sounding data), averaging the calculations from

[4] We also interpolated ECMWF-based CPT properties at Kapingamarangi from values at the four nearest ECMWF grid points. The interpolated properties are almost the same as those at the nearest ECMWF grid.

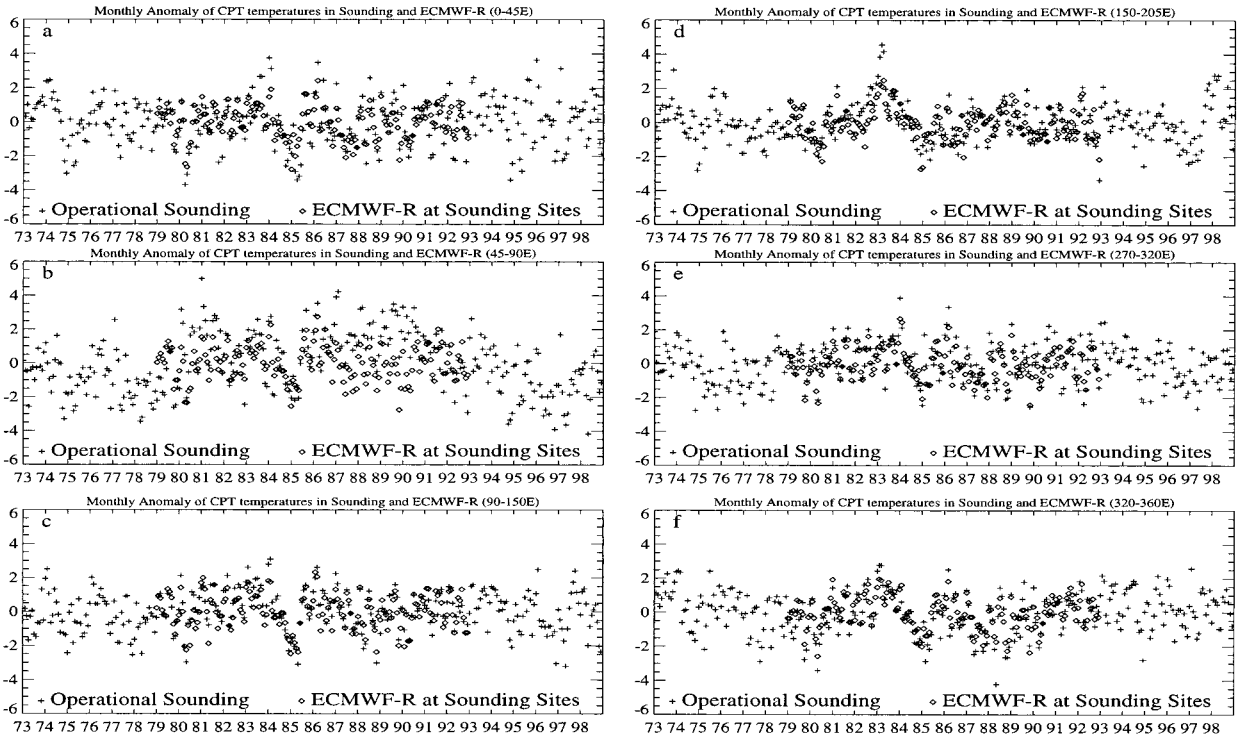

FIG. 2. Comparison between ECMWF-based monthly regional CPT temperature anomalies (open diamonds) and monthly regional CPT temperature anomalies from the operational soundings (plus sign) in six tropical regions. The temperature anomalies are residuals after the seasonal cycles and the secular trends are removed, and units of the temperature anomalies are Kelvin. (a)–(f) R1, R2, R3, R4, R6, and R7, respectively.

all sounding profiles. To reduce the possible impact of sampling differences, we first interpolated the ECMWF-based CPT calculations to the sounding stations, then sampled the resulting data on the dates when the sounding stations measured the CPT, and finally averaged the sampled data to get regional monthly means in the same way as was done with the operational soundings. The regional monthly CPT temperature and pressure anomalies (about the seasonal cycle and the secular trend), derived from ECMWF reanalyses during the period 1979–93 and from the operational soundings during the period 1973–98, are shown in Figs. 2 and 3. ECMWF reanalyses track the interannual variability of CPT temperatures and pressures in operational soundings quite well in all regions (though relatively poor in region R2). Even though it is expected that the quality of the reanalyses should be better in data-rich regions than that in data-sparse regions, Figs. 2 and 3 show that the bias features in the reanalyses at the tropopause level are similar in these regions. The interannual variations of CPT temperatures and pressures are positively correlated. Cold CPT temperature anomalies correspond to negative CPT pressure anomalies and vise versa.

We also applied the cubic spline method to map CPT temperatures, using both monthly mean NCEP and ECMWF reanalyses. These results are shown in Fig. 4 for January 1991, and they largely agree with those of Newell and Gould-Stewart (1981) in that the coldest temperatures are found over the warm pool region. The ECMWF temperatures are found to be about 2 K cooler than those from NCEP. This makes a big difference in the calculation of the SMR of water vapor. Listed in Table 1 are monthly mean CPT temperatures for three months from the TOGA COARE soundings at Kapingamarangi (KAP), ECMWF daily reanalysis products, and NCEP monthly mean reanalysis products at the nearest grid point (155°E, at the equator). The SMRs in ppmv corresponding to these temperatures are listed in the parentheses in Table 1 assuming the pressures were 100 mb. It can be seen that the NCEP CPT is too warm, about 4–5 K warmer than the KAP sounding. ECMWF reanalyses are colder than those of NCEP reanalyses by a few degrees and are in closer agreement with the sounding observations, although ECMWF reanalyses still contain a one-side warm bias. The CPT temperature difference between ECMWF reanalyses and NCEP reanalyses is consistent with the results by Pawson and Fiorino (1998) who compared the 100-mb temperature reanalyses for 1979–93 produced by ECMWF and NCEP. Randel et al. (1999) have demonstrated the one-side warm bias in the NCEP reanalyses.

The work of Newell and Gould-Stewart (1981) has been extended in two ways. We have looked at the tropical CPT, rather than the 100-hPa temperature maps, and

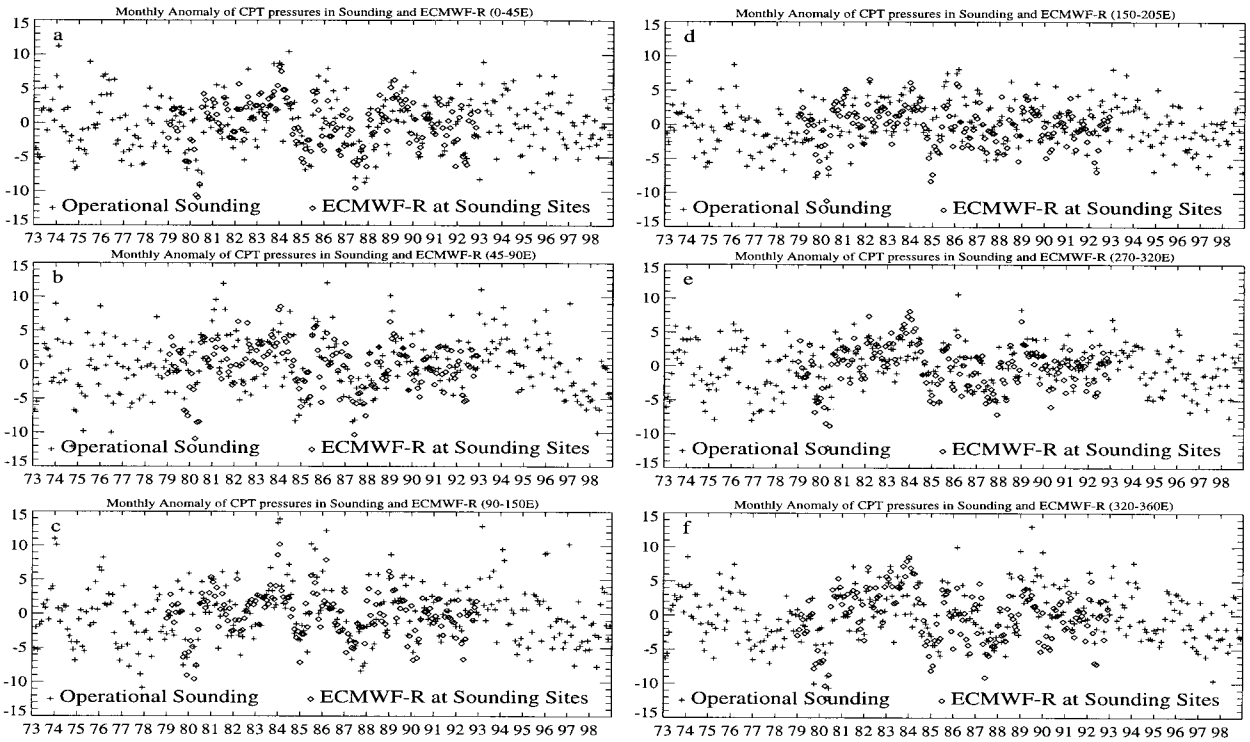

FIG. 3. As for Fig. 2 except for pressure anomalies. Units of the pressure anomalies are mb.

we have looked at the effects of daily variations within a month rather than just examining monthly mean conditions. The tropical minimum SMR locations on a daily basis for 1979–93 have been plotted according to the ECMWF-based calculations, and Fig. 5 shows the scatter for 1986–90. A common feature of the seasonal cycle in the scatter of the tropical minimum SMR locations can be summarized by the last row in Fig. 5. In January, these points are mainly clustered in the warm pool region, consistent with the results of Newell and Gould-Stewart (1981). In April, however, these points, while still having their maximum concentration in the warm pool region, are distributed more broadly in longitude. In July, these points are distributed still more broadly in longitude than in January, but in addition one clearly sees the northward displacement of the cold-point tropopause locations to the north in the Indian summer monsoon region. The main part of the stratospheric fountain is still over the western Pacific. This has not been reported in previous studies. Finally, in October,

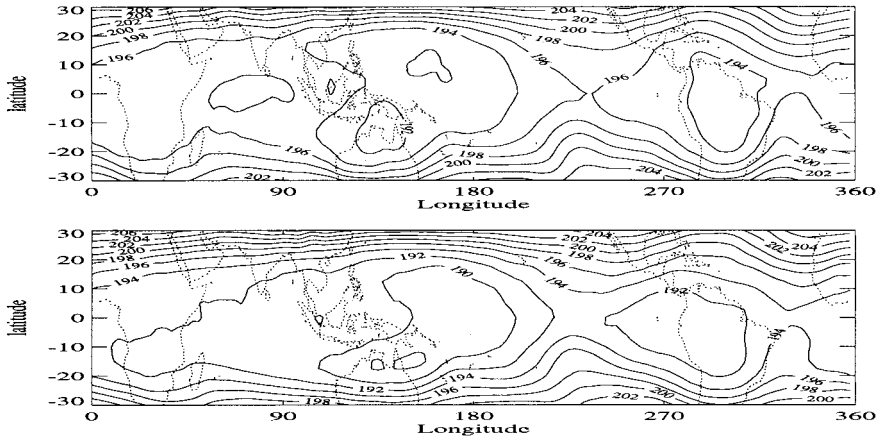

FIG. 4. Monthly mean temperature at the CPT for Jan 1991 as calculated from (top) NCEP reanalysis and (bottom) ECMWF reanalysis by using cubic spline interpolation. Contour interval is 2 K.

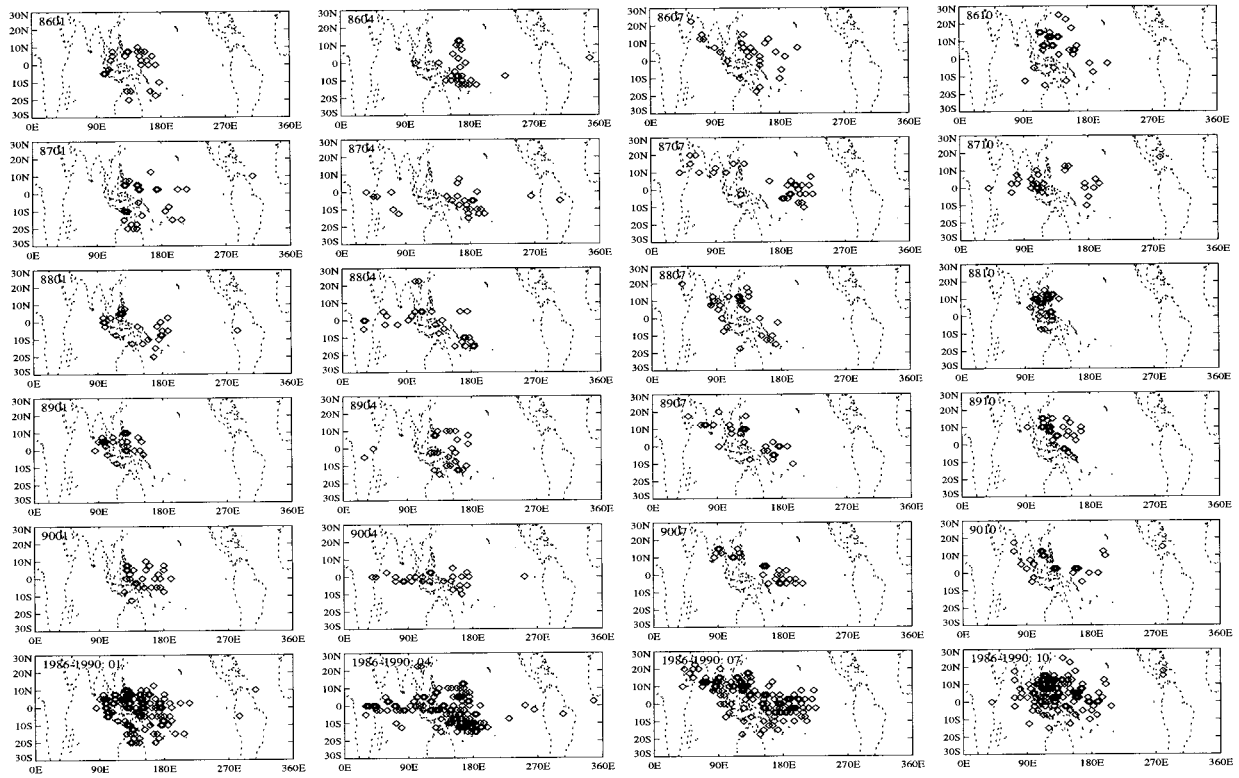

FIG. 5. Locations of daily minimum SMRs. From left to right are Jan, Apr, Jul, and Oct. From top to bottom are for years 1986, 1987, 1988, 1989, 1990, and 5-yr combination (1986–90).

one sees a contraction of the region of cold-point tropopause locations toward the January picture. In general, the results of Fig. 5 show some consistency with the Newell and Gould-Stewart (1981) picture but also show more longitudinal spread, consistent with the results of Atticks and Robinson (1983) and Frederick and Douglass (1983); and clearly show the influence of the Indian summer monson on the stratospheric fountain.

It can be seen in Fig. 5 that the locations of daily minimum SMRs spread wider in longitude during the El Niño event (August 1986–February 1988) than during the La Niña event (May 1988–Jun 1989). The daily minimum SMRs at the tropical CPT tended to occur more frequently over the central Pacific during the El Niño event. The interannual variabilities will be further discussed in the next section.

3. Low-frequency variabilities of the tropical CPT

We averaged the ECMWF reanalyses based daily CPT calculations to obtain monthly CPT temperatures, pressures, and heights. We have calculated power spectra using monthly mean time series at many tropical grids and found that the power spectra of the tropical CPT properties at most longitudes show three peaks (e.g., Fig. 6). Besides the dominant seasonal cycle, there are two other principal variabilities in the tropical CPT. One corresponds to a period of about ½ yr, and the other corresponds to a band of low-frequency variabilities with periods about 2–7 yr.

The stratospheric QBO and tropospheric ENSO are two of the dominant low-frequency variabilities in the Tropics. Some influence of the QBO and the ENSO on the lapse rate tropopause has been reported using data from sparse sounding stations (Reid and Gage 1985; Gage and Reid 1987; Reid 1994). However, the relationship of the tropical *cold point tropopause* with the QBO and/or the ENSO has never been previously reported, let alone over the entire Tropics. To further investigate the influences of the QBO and ENSO on the tropical CPT, we define CPT ''anomalies,'' $\epsilon(t)$, as the residual after the seasonal cycle and secular trend have been removed.

The zonal wind shear at 50 mb (difference between the winds at 40 and 70 mb) over Singapore and the SSTA in the Niño-3.4 region are used as reference indices to extract the low-frequency variabilities in CPT, which may be related to the stratospheric QBO and tropospheric ENSO, respectively. CPT anomalies were divided into two groups according to the sign of the wind shear, and were divided into two groups according to El Niño and La Niña events, which were defined following the definition in Trenberth (1997). The composite analyses of CPT properties with respect to the wind shear at 50 mb show strong zonal asymmetry,

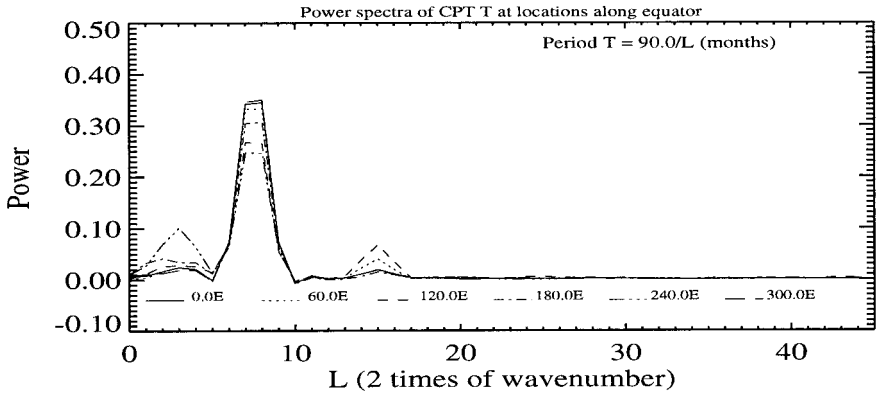

FIG. 6. Power spectra of standardized monthly mean CPT temperatures, with secular trends removed, at 6 ECMWF grid points along the equator.

which is in apparent contradiction to the fact that the stratospheric QBO is predominantly zonally symmetric (Andrews et al. 1987; Yulaeva and Wallace 1994) and implies that these composites possibly may be contaminated by the ENSO variabilities. Contamination by the QBO can be seen in the composite analyses with respect to the ENSO events (figures not shown).

As a first step to separate the influences of the QBO and ENSO on the tropical CPT, we examined their lag correlations. The lag-correlations between the wind shears at 50 mb and the CPT temperatures indicated that stratospheric zonal wind shears at 50 mb have significant correlation with CPT temperatures at a time lag of -10 (± 2) or $+6$ (± 2) months (figures not shown, but they have similar patterns to those of Fig. 7).[5] If the wind shears at 50 mb lag the CPT temperatures by 10 months, the correlation coefficients between the wind shears and CPT temperatures are negative almost everywhere in the Tropics. If the wind shears at 50 mb lead by 6 months, the stratospheric wind shears and CPT temperatures are positively related. The difference of these lags happens to be about half the period of the stratospheric QBO. This is likely an indication of the quasi-periodic impact of the stratospheric QBO. The main features in the maps of the correlations between the CPT properties and the QBO wind shear are zonally symmetric. The correlation analyses of the SSTA in the Niño-3.4 region and the CPT indicated that the best correlation occurs at 0 time lag (figures not shown, but they have similar patterns to those of Fig. 8). The correlation maps between the SSTA in the Niño-3.4 region and the tropical CPT properties show a dipole feature.

Mathematically, the SSTA and the QBO are not independent due to the overlap in their frequency domain. A quasi-biennial oscillation in SST has been noted although it has not been thought to be physically related to the stratospheric QBO (Xu 1992; Meehl 1993; Ropelewski et al. 1992). Geller et al. (1997), however, found that the stratospheric QBO might be related to SST variations in a nonlinear fashion. Investigating the physical connection between the QBO and SST is beyond the scope of this paper. In order to separate the influences of the stratospheric QBO and the tropospheric ENSO on the tropical CPT, we have made two independent QBO and SSTA time series using a Butterworth bandpass filter (Hamming 1989). The response function of the bandpass filter we used has the value 1 at a period of 28 months, and ½ at periods of about 22 and 34 months. We used this to extract the quasi-biennial variabilities from the wind shears at 50 mb over Singapore. For the SSTA, we subtracted bandpassed time series from the SSTA anomalies. The above process can be expressed mathematically by the following:

$$\mathrm{QBO}(t)' = \mathrm{QBO}(t)_{22-34m} \quad (1)$$

$$\mathrm{SSTA}(t)' = \mathrm{SSTA}(t) - \mathrm{SSTA}(t)_{22-34m}, \quad (2)$$

in which the QBO(t) and SSTA(t) are stratospheric wind shear anomalies at 50 mb and surface temperature anomalies in the Niño-3.4 region (note that all trends have been removed), $\mathrm{QBO}(t)_{22-34m}$ and $\mathrm{SSTA}(t)_{22-34}$ are the quasi-biennial components in the stratospheric wind shear anomalies at 50 mb and the surface sea temperature anomalies in the Niño-3.4 region, and QBO(t)′ and SSTA(t)′ are the new QBO wind shear and SSTA time series, respectively. QBO(t)′ is almost identical to the original time series QBO(t). The quasi-biennial oscillation in SSTA(t) accounts for about 30% of the total

TABLE 1. Monthly mean CPT temperatures and (SMRs).

	KAP	ECMWF	NCEP
Dec 1992	184.61 (2.03)	188.45 (2.73)	189.54 (2.96)
Jan 1993	188.19 (2.67)	189.73 (3.00)	192.88 (3.77)
Feb 1993	190.16 (3.10)	191.63 (3.45)	193.95 (4.07)

[5] Correlation coefficients are significant at 95% in most parts of the Tropics according to the method of Oort and Yienger (1996).

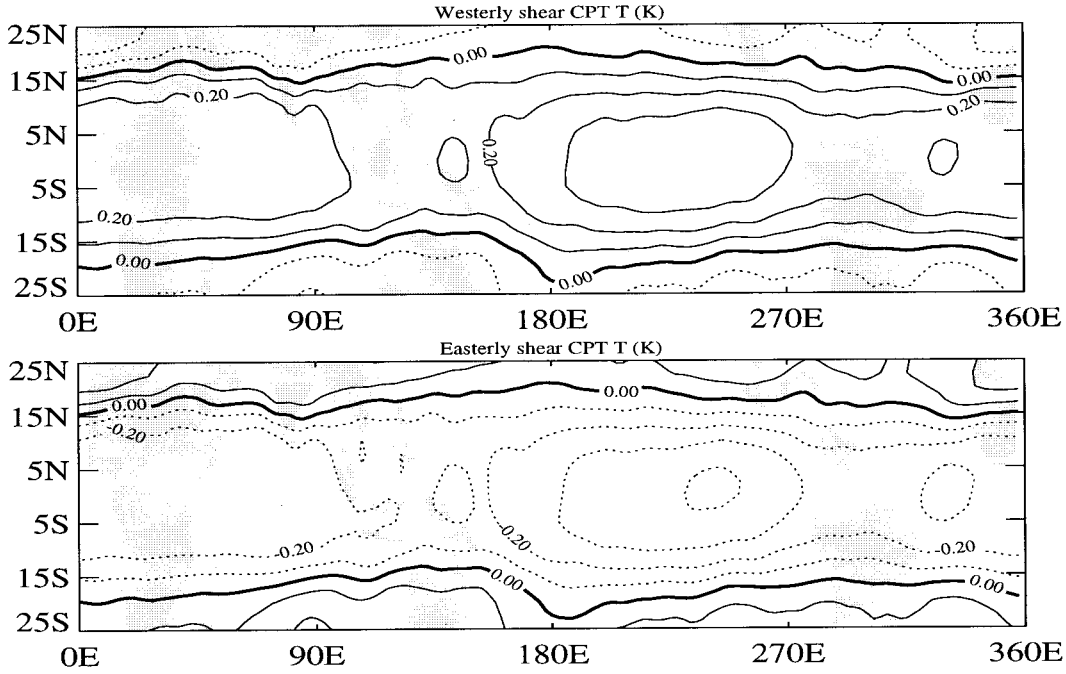

FIG. 7. Composite analyses of CPT temperatures under westerly and easterly stratospheric zonal wind shear conditions. Note that the shears lead the CPT temperatures by 6 months. Contour interval is 0.10 K.

variance of the SSTA(t), so SSTA(t)′ still contains much of the information about the SSTA even when its quasi-biennial oscillations have been deleted.

QBO(t)′ and SSTA(t)′ are mathematically independent of each other and they can be applied in the bivariate regression to separate the influences of the stratospheric QBO and the tropospheric ENSO on the tropical CPT,

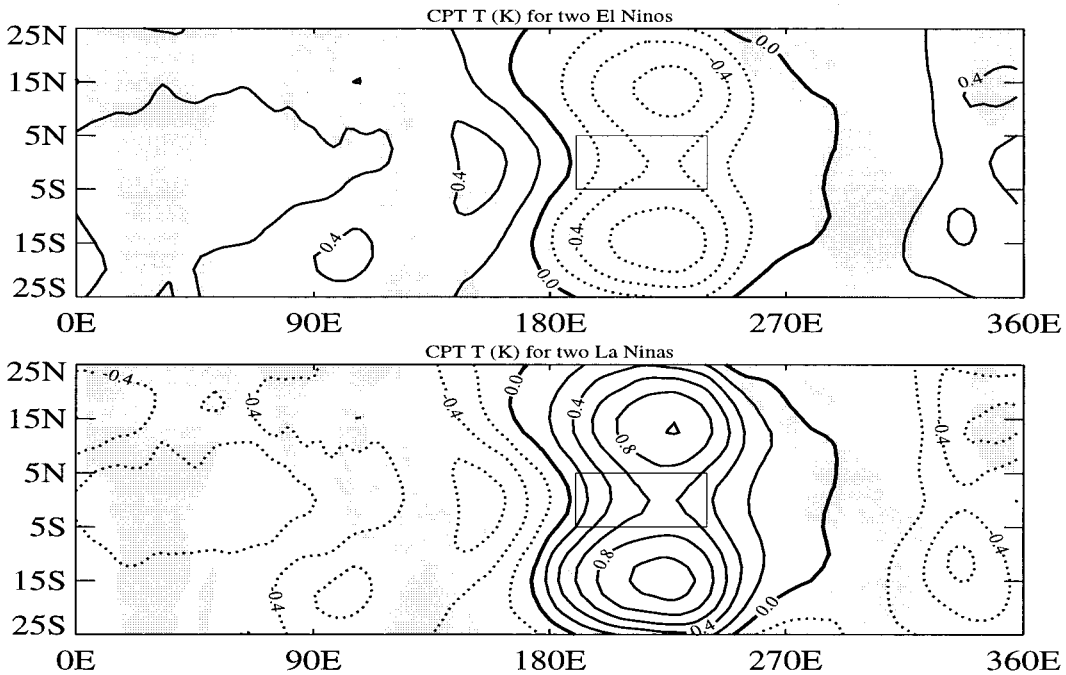

FIG. 8. Composite analyses of CPT temperatures during two ENSO events that occurred during 1979–93. See the text for the selection of ENSO events. Square boxes show the Niño-3.4 region. Contour interval is 0.20 K.

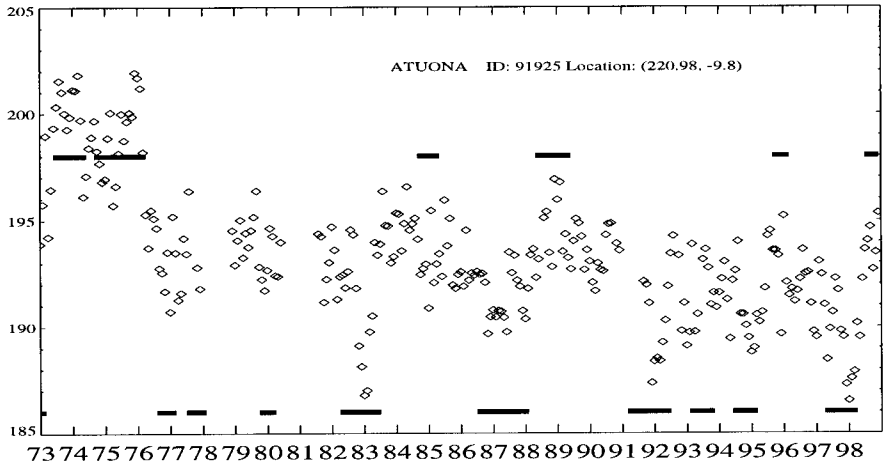

FIG. 9. Monthly mean CPT temperatures at a sounding station close to Niño-3.4 region. The station ID and location (long, lat) are shown in the figure. The El Niño and La Niña events, following the definition of Trenberth (1997), are indicated by lower solid lines and upper solid lines, respectively.

$$\epsilon(t) = a \times \mathrm{QBO}(t-6)' + b \times \mathrm{SSTA}(t)' + \gamma(t), \quad (3)$$

in which $t - 6$ appears rather than t, because of the lag between the QBO wind shear at 50 mb and the CPT temperatures. Using $t + 10$ instead of $t - 6$ is equivalent to a change of sign for a in Eq. (3). This regression implicitly assumes that the quasi-biennial component in SSTA does not contribute significantly to the variability of the CPT properties or affects the tropical CPT in a way different from the way in which the stratospheric QBO influences the tropical CPT. In other words, the effect of the quasi-biennial component in the SSTA on the CPT temperatures has been put into $\gamma(t)$. To ensure that the QBO′ and SSTA′ have the same weights in the regression, the time series of $\mathrm{QBO}(t-6)'$ and $\mathrm{SSTA}(t)'$ in the Eq. (3) are normalized.

We have produced composite analyses using the regressed time series $a \times \mathrm{QBO}(t-6)'$ and $b \times \mathrm{SSTA}(t)'$. The zonally symmetric features of the QBO in CPT properties are clearly shown in the composite analysis of the CPT temperatures for the westerly and easterly QBO wind shears (Fig. 7). During the westerly shear period, the composited tropical CPT is warmer by 0.2 to 0.3 K, and during easterly shear conditions it is colder by 0.2 to 0.4 K. Consistently, the CPT pressure is larger and the CPT height is lower under westerly shear conditions, and the CPT pressure is smaller and the CPT height is higher under easterly shear conditions (figures not shown). The largest temperature anomaly occurs over the eastern Pacific, while the largest pressure or height anomaly occurs over the western Pacific. This is consistent with the 28-month oscillation fittings of the tropical CPT properties (figures not shown). There seems to be a stationary wave with wavenumber 2 superposing on a zonally homogeneous field (Fig. 7), for example, there are minima over the western Pacific and the southern America. However, this asymmetry might be due to the fact that the influences of the QBO and ENSO on the tropical CPT can not be perfectly separated.

Figure 8 shows the composites of the CPT temperature anomalies for two El Niños and two La Niñas that occurred during 1979–93 (the two El Niños occurred during April 1982–July 1983 and August 1986–February 1988, and the two La Niñas during September 1984–June 1985 and May 1988–January 1989). The temperature anomalies associated with ENSO are larger than those associated with the QBO. They can be as low as −0.6 K during El Niño and as high as 1.0 K during La Niña over the eastern Pacific. The temperature anomalies over the western Pacific are about 0.4 K (−0.4 K) during El Niño (La Niña) events. It seems the CPT temperature anomalies associated with the ENSO are slightly stronger in the southern hemispheric Tropics than in the northern hemispheric Tropics. The CPT temperature anomalies are relatively weak over the tropical Africa and the western Indian Ocean and seem not well related with the ENSO. Similar results were found by Yulaeva and Wallace (1994). Figure 8 shows three distinct features. First, there is an east–west (E–W) dipole over the tropical Pacific. The second feature is that there are three north–south (N–S) dumbbells in the Tropics. The strongest dumbbell is over the central to eastern Pacific. One dumbbell pattern is clear over the Atlantic, and similar features are also seen over the eastern Indian Ocean and the western Pacific, though less clearly. The third feature is that there is a maximum (in absolute value) over the equatorial western Pacific. These three features can be explained by changes of tropical convection activity associated with ENSO as will be discussed further in the next section. Similar features of the CPT variabilities associated with ENSO also can be seen in the pressure and height composites (figures not shown), although those features are not as clear as the temperature composites. Composite analyses based on

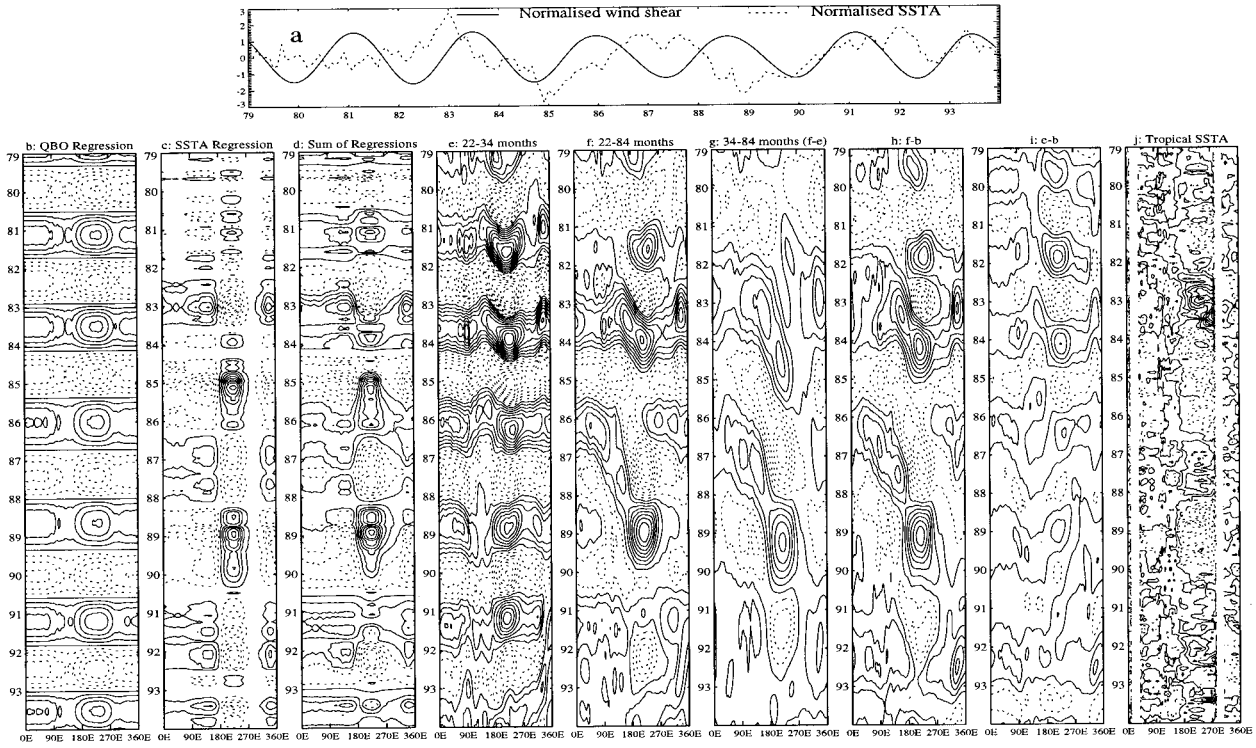

FIG. 10. (a) The normalized time series of the stratospheric zonal wind shear at 50 mb over Singapore (6-month lag shifted) and SSTA in the Niño-3.4 region, which were used in Eq. (3). (b), (c), and (d) The QBO wind shear regressions in CPT temperatures, SSTA regression in CPT temperatures, and their sum, respectively. (e) and (f) show the CPT temperature anomalies in the period bands of 22–34 months and 22–84 months, respectively. (g) The difference between (f) and (e). (h) The difference beween (f) and (b). (i) The difference between (e) and (b). (j) The tropical mean (5°S–5°N) SSTA. CPT temperature anomalies were averaged over 15°S–15°N. Contour intervals are 0.1 K for (b) and (e), 0.5 K for (j), and 0.2 K for the others. Negative contours are dashed. Note that the contour 0 is dismissed in (c) and the first solid contour is 0.1 K.

the regressed time series have been performed for each ENSO event. The results for the composites of each ENSO event look almost the same as that shown in Fig. 8 except for slight differences in magnitude.

The QBO and ENSO signatures in the tropical CPT shown in Figs. 7 and 8 are in agreement with EOFs 1 and 2 of the tropical stratospheric temperature anomalies observed by the lower-stratospheric channel of the Microwave Sounding Unit (MSU-4; Fig. 17 in Yulaeva and Wallace 1994). This indicates that the QBO and ENSO signatures in the tropical CPT found here is reliable even in the region where sounding observations are sparse or even not available.

A station (Atuona) in our operational sounding dataset has its location (220.98°E, 9.8°S) close to the Niño-3.4 region (Fig. 9). The extreme warm CPT temperatures during 1973–76 may have been caused by a change of instrument, or may be partially due to the two La Niña events that occurred during that period. It can be seen that the CPT temperature over that station has a close relationship with ENSO, colder in El Niño events and warmer in La Niña events in 1976–98. It is very interesting that the CPT temperatures during 1982–83 were colder than those in 1986–88, reflecting the difference in strength between the two El Niño events that occurred around 1983 and 1987. During strong El Niño events (e.g., 1982–83 and 1997–98 El Niños) the CPT temperatures were about 5 K colder than normal. The normal annual cycle of the tropical tropopause temperature has the tropopause colder and higher in Northern Hemispheric (NH) winter due to stronger extratropical wave forcing and warmer and lower in NH summer due to weaker wave forcing (Yulaeva et al. 1994). However, in some NH winters during La Niña events (e.g., 1988–89 NH winter) the CPT was very warm, even a few degrees warmer than normal NH summertime CPT temperatures. The CPT temperature also warmed up during the recent La Niña event, which started in July 1998.

Observations from sounding stations in the maritime continent in the western Pacific show some indications of opposite variation of the tropical CPT temperature during ENSO events (figure not shown), that is, colder CPTs over the western Pacific during La Niña events and warmer during El Niño events. This is consistent with the picture of changes of convection and longitudinal circulation during ENSO events.

The QBO in the tropical CPT is predominantly zonally symmetric, with an amplitude of about 0.2–0.4 K (Fig. 10b). In contrast, the ENSO-like variabilities in the tropical CPT are very zonally asymmetric (Fig. 10c).

The SSTA regression of the tropical CPT temperatures was very weak during 1979–81. This is because that there was only one short and weak El Niño event and no La Niña event during that period. Strong anomalies occurred after April 1982. The presence of the El Niño and La Niña events implies changes in the longitudinal circulation, in the sense of an anomaly. During La Niña events, the enhanced upward branch of the Walker circulation is over the western Pacific and convection is relatively stronger there. The enhanced downward branch of the Walker circulation is over the eastern Pacific and convection is relatively weaker there. Correspondingly, the CPT is colder over the western Pacific and warmer over the eastern Pacific. During El Niño events, the enhanced upward branch of the longitudinal circulation (i.e., the Walker circulation during this period) is over the central to eastern Pacific so that the CPT is colder there and the enhanced downward branch is over the western Pacific so that the CPT is warmer there.

Interference between the stratospheric QBO and tropical ENSO can be seen in Fig. 10. During the 1982–83 El Niño, the QBO wind shears lagged about ¼ period (after a 6-month shift, Fig. 10a), and the QBO in CPT temperatures was changing from negative anomalies to positive anomalies (Fig. 10b). During the 1986–88 El Niño, QBO wind shears were out of phase with the SSTA, and the QBO in CPT temperatures was of the same sign as the SSTA regression of CPT temperature, so the sum of the regressions was enhanced. The situation was opposite during the El Niño, which occurred in 1993 so that the SSTA regression of CPT temperature was almost canceled by the QBO regression (Fig. 10d).

To examine the propagation of tropical CPT temperature anomalies along the equator and to examine how good the regressions are, we performed Fourier harmonic analysis upon the tropical CPT temperatures, and summed up harmonic components with periods between 22 and 34 months (QBO characteristic periods) and between 22 and 84 months (the main periods for the SSTA). Their tropical averages (averaged over 15°S–15°N) are shown in Figs. 10e and 10f and their difference is shown in Fig. 10g. For reference, the tropical mean SSTA (average over 5°S–5°N) is shown in Fig. 10j. The zonal symmetry of the stratospheric QBO influence on the tropical CPT can be seen in Fig. 10e; however, some zonal asymmetry is evident and it might be from the effect of the quasi-biennial oscillations in the SSTA. Figure 10g is the difference between Figs. 10f and 10e, that is, corresponding to variabilities with periods of 34–84 months. In this figure, CPT temperature anomalies over the eastern Pacific during the 1982–83 El Niño were mostly positive and were positive during the El Niño, which occurred in 1993, unlike that during 1986–88 El Niño and 1991–92 Niño. The warmer CPT temperatures in the 1982–83 El Niño may be due to the warming effect of the eruption of El Chichon (Angell 1993). Figure 10h shows the difference between the sum of the harmonic components with periods of 22–84 months and the QBO regression, and it approximately represents the influence from ENSO only. The anomalies during the 1982–83 El Niño in Fig. 10h were more like those during the 1986–88 El Niño than in Fig. 10g. The anomalies over the eastern Pacific in Fig. 10h are negative and as strong as in the 1986–88 El Niño. Also, during the 1993 El Niño, the anomalies over the eastern Pacific were slightly negative in Fig. 10h, although they were positive in Fig. 10f. Comparing Figs. 10h and 10f with 10j, respectively, we find that the correlation between the CPT temperatures and the SSTA over the Pacific becomes stronger when the influence of the stratospheric QBO is suppressed.

The influence of the quasi-biennial oscillation in SSTA on the tropical CPT temperatures can be estimated by the difference between the sum of the harmonic components with periods 22–34 months and the QBO regression of the tropical CPT temperatures (Fig. 10i). The QBO in the tropical CPT induced by the quasi-biennial oscillation in the SSTA is zonally asymmetric and was stronger during 1979–85 and weaker during 1986–93. It is interesting that both the variabilities of CPT temperatures in the period band 34–84 months and the QBO in CPT temperatures induced by the quasi-biennial oscillation in SSTA during the 1982–83 El Niño were different from those during the 1986–88 El Niño.

4. Discussion

a. Comparison with recent work

Examining the statistical significance of the previous regression analyses is very difficult. However, our results are supported by the analyses made by Randel et al. (2000) using the NCEP reanalyses. As we were writing this paper, we obtained a copy of of ''interannual variability of the tropical tropopause derived from radiosonde data and NCEP reanalyses'' by Randel et al. (2000). Although NCEP reanalyses have a larger one-side warm bias than ECMWF reanalyses, NCEP reanalyses can also track tropopause variability. Common findings in their analyses and our results are that the QBO in the tropical tropopause is zonally symmetric and that ENSO relevant variabilities in the tropical tropopause have dipole features. However, there are some differences between our analyses and theirs. First, the tropopause in their paper is a lapse rate tropopause, and we applied the CPT definition. This latter tropopause definition is more relevant to STE and the coupling between the tropical stratosphere and the tropical troposphere, but using the lapse rate tropopause definition allowed them to obtain QBO and ENSO influences on the extratropical tropopause. Second, they found a simultaneous correlation between the stratospheric QBO and their lapse rate tropopause temperatures; however, we found that the stratospheric QBO leads the ECMWF based CPT temperature by 6 months. They used the

stratospheric zonal wind at 50 mb over Singapore as the index for stratospheric QBO, and we used the wind shear at 50 mb over Singapore, however. This difference probably explains the second difference just mentioned. Finally, they have to first remove the zonal mean in order to obtain a clear ENSO influence on the tropical tropopause. This is not needed in our analysis. However, we have to suppress the interference from the stratospheric QBO to get the ENSO fingerprints in the tropical CPT.

b. Mechanism for ENSO signature in CPT

The annual cycle of the zonal mean tropical tropopause is driven by extratropical stratospheric wave forcing (Yulaeva et al. 1994), but the zonal asymmetrics in the tropical tropopause can be attributed to the direct response of the atmosphere to a large-scale region of tropospheric diabatic heating (Highwood and Hoskins 1998). The mechanism is summarized in Fig. 9 in Highwood and Hoskins (1998), an extended framework of Gill model (1980). Briefly speaking, there is ascent motion, with a horizontal scale larger than that of convection, in the upper troposphere and the lower stratosphere, which is forced by diabatic heating in the troposphere. Thus, the stronger diabatic heating or convection, the colder the tropopause. This hypothesis was supported by results from a baroclinic model with imposed diabatic heating (Highwood and Hoskins 1998). A few observations can be found in Teitelbaum et al. (2000), which show the *instantaneous* relationship between the CPT and the convection. The mechanism proposed by Highwood and Hoskins (1998) can be extended to explain the simultaneous anti-correlation between the SSTA and the CPT temperatures over the eastern Pacific. During El Niño events, the active convection center shifts to the central to eastern Pacific. As a result, there is more precipitation in the central to eastern Pacific and so more diabatic heating there. Thus, during El Niño events, the tropopause is colder over the eastern Pacific. During La Niña events, the situation is reversed. The propagation of the region of colder CPT temperatures from the western Pacific to the eastern Pacific is consistent with the propagation of the region of positive SSTAs, and supports the above mechanism (see Fig. 10h). The position of the dumbbell over the eastern Pacific is consistent with the pattern of the 200-mb streamfuction anomalies forced by diabatic heating below over the equator (Arkin 1984). This provides additional evidence for the role of convection in determining the low-frequency variabilities in the tropical CPT.

Yulaeva and Wallace (1994) investigated the signature in global temperature and precipitation fields derived from the Microwave Sounding Unit (MSU). The ENSO-associated temperature anomalies in the troposphere (MSU-2) and the lower stratosphere (MSU-4) are very consistent with the ENSO signature in the tropical CPT, in respect of the shape and positions of the E–W dipole and N–S dumbbells and the maximum anomaly over the western Pacific.[6] The ENSO has a coherent vertical structure in the tropical atmospheric temperature, which reverses sign at certain altitude below the CPT. For instance, during El Niño events, the tropical troposphere (1000–200-mb layer) over the eastern Pacific is warmer and the tropopause and the lower stratosphere is colder. During El Niño events, distribution of the tropical tropospheric temperature anomalies looks like Fig. 8b (or Fig. 9b in Yulaeva and Wallace 1994) and distribution for the tropopause and the lower stratosphere looks like Fig. 8a (or Fig. 17b in Yulaeva and Wallace 1994). Zhou and Sun (1994) extended the Gill model (Gill 1980) including a cooling over the western domain and a heating over the eastern domain to study the tropical tropospheric nonlinear steady response to two heating sources of contrasting nature. Outgoing longwave radiation (OLR) observations indicate positive anomalies (negative diabatic heating anomalies) over the eastern Indian Ocean and the western Pacific and negative anomalies (positive diabatic heating anomalies) over the central to eastern Pacific (Yulaeva and Wallace 1994). Thus, the distribution of two idealized heat sources considered by Zhou and Sun (1994) represents the longitudinal distribution of major diabatic heating anomalies in the Tropics during El Niño events. The steady geopotential height response at the top of model domain to these two heat sources of contrasting nature shows that there is positive dumbbell over the eastern half domain and a negative dumbbell over the western half domain. These positive and negative dumbbells form an E–W (positive–negative) dipole. Additionally, there is a negative maximum geopotential height anomaly to the east of the western cooling source and this maximum anomaly is a result of wave–wave interaction (Zhou and Sun 1994). Thus, the geopotential height response to W–E negative–positive paired heating sources is hydrostically consistent with Fig. 8a, which shows the El Niño associated tropical CPT temperature anomalies. However, the response of the temperature anomaly was assumed to have the same vertical structure as the heating (Gill 1980; Zhou and Sun 1994). The Gill model needs to be extended further, for example, including a stratospheric layer or following the framework presented in Highwood and Hoskins (1998), to explain the ENSO signature in the tropical CPT temperature more reasonably though results from this model have shown that the E–W dipole feature in the ENSO signature in the tropical CPT is caused by the changes in tropical convection during ENSO events, the N–S dumbbell feature is due to rotation of the earth, and the maximum over the equatorial western Pacific

[6] Yulaeva and Wallace (1994) also found a zonally homogeneous ENSO signature in the tropical tropospheric temperature which lags the SST by about 3 months.

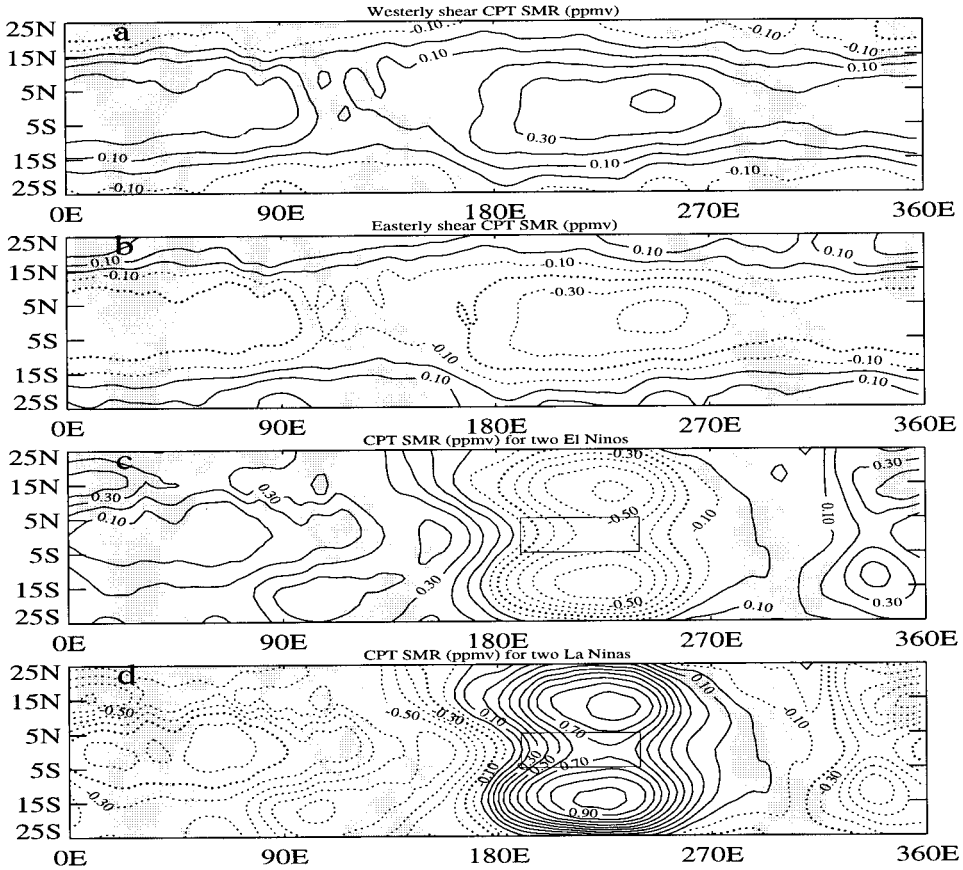

FIG. 11. Composite analyses of the tropical CPT SMR for QBO westerly shears at 50 mb over Singapore (a); easterly shears (b); the 1982–83 and 1986–88 El Niños (c); and the 1984–85 and 1988–89 La Niñas (d), using the regressed time series in Eq. (3). Contour intervals are 0.10 ppmv.

is caused by nonlinear wave–wave interaction (Zhou and Sun 1994).

As mentioned in the introduction, we have found that the tropical CPTs were cooling everywhere in the Tropics during 1973–98. Consistently, tropical SST is warming, and tropical OLR is decreasing. Waliser and Zhou (1997) indicated that the tropical OLR decreasing trend is consistent with the increasing trend in tropical in situ rainfall observations. It is reasonable to hypothesize that the changes in tropical convection due to the warming SST might be responsible for the cooling trend in the tropical CPT (Zhou et al. 2001; Zhou 2000).

In summary then, tropical convection variability plays an important role in determining the low-frequency variability of the tropical CPT, including the secular trend.

c. Mechanism for QBO signature in CPT

Tropical stratospheric QBO is a significant low-frequency variability and has been intensively investigated for decades (e.g., Reed et al. 1961; Veryard and Ebdon 1961; Plumb and Bell 1982; Naujoket 1986). Our analysis indicated that the westerly shears at 50 mb, which are accompanied by warm temperature anomalies (Plumb and Bell 1982), lead the tropical CPT temperatures by about 6 months and are positively correlated with the tropical CPT temperatures. It takes about 3–4 months for the westerly shear at 50 mb to reach 100 mb and takes about 7 months for the easterly shear to propagate from 50 mb to 100 mb (Naujoket 1986), which gives an average of about 5–6 months. This time lag is very consistent with our analyses. The amplitude of QBO temperature perturbation can be estimated using

$$f_0\overline{u}_z + H^{-1}R\overline{T}_y = 0, \tag{4}$$

which is Eq. (7.1.1d) of Andrews et al. (1987). Given a wind change over a scale height $\Delta\overline{u} = 10$ m s^{-1} and a latitudinal scale $L = 1000$ km, Eq. (4) gives an estimate of about 0.79 K for temperature change over a distance L. Amplitude of the CPT temperature anomalies associated with the QBO is about 0.3–0.5 K (Fig. 10b). Consistency in time lag and amplitude suggests that the QBO signature in the tropical CPT temperatures is probably due to the stratospheric QBO temperature

anomalies that accompany the downward-propagating QBO meridional circulation.

The annual cycle of the zonal mean tropical tropopause is driven by extratropical wave forcing (Yulaeva et al. 1994), however, the extent to which the extratropical wave forcing affects the low-frequency variabilities of the tropical tropopause is unknown. Surely, some of the QBO effect is affected by the extratropical wave forcing and some might be driven by the QBO meridional circulation. Future studies of the low-frequency variations of the tropical CPT should consider the stratospheric QBO, the tropospheric ENSO, and the extratropical wave forcing at the same time.

d. Entry value of water vapor

Since the upward flux from the troposphere into the stratosphere mainly occurs in the Tropics (Holton et al. 1995), one may estimate the entry value of water vapor mixing ratio purely from measurements of water vapor at the tropical tropopause. However, this method is subject to serious sampling errors and large spatial and temporal variabilities of measurements near the tropical tropopause. Most estimations of the entry value have been indirectly inferred from middle latitude stratospheric measurements (e.g., Abbas et al. 1996), and the focus has been on the annual mean only.

Randel et al. (2000) have performed multivariate regression using sounding data from 12 tropical sounding stations, and found that the structures of the QBO and ENSO effects on the tropical lapse rate tropopause derived from soundings are similar to the structures derived from the NCEP reanalyses. As proved in section 2, the ECMWF reanalyses track the CPT variabilities in sounding data very well. Thus, the influences of the QBO and ENSO on the tropical CPT are of good reliability. Since the Clausius–Clapeyron equation is strongly nonlinear (Reid and Gage 1996; Zhou and Geller 1998), small changes in the temperature can make a large difference in the resulting saturation mixing ratio. The amplitudes of both the QBO and ENSO fingerprints in tropical CPT temperatures are large enough to yield significant variations in the SMR at the tropical CPT (Figs. 7–10). Composites for the CPT SMRs have the same features in the CPT temperature composites (Fig. 11). This is because the SMR is more dependent on temperature than on pressure. The amplitudes of the variations of the CPT SMR due to the stratospheric QBO are about 0.1–0.4 ppmv. The composite anomalies of the CPT SMR are about −0.6–0.4 ppmv during the El Niño events, and −0.6–0.9 ppmv during La Niña events. Because of the dryness of the tropical lower stratosphere (about 3–5 ppmv), the anomalies shown in Fig. 11 are not small. In addition, the amplitudes of the variabilities in the CPT SMR due to the effects of the QBO and ENSO are larger than the composite anomalies shown in Fig. 11, which are means over the corresponding periods. This can be seen in a longitude–time evolution figure, such as Fig. 10 but for the CPT SMR (figure not shown). Also, we have found that the tropical CPT has been cooling at a rate of -0.57 K decade^{-1}. Corresponding to this cooling trend in the CPT temperatures and a decreasing trend in the CPT pressures, there is a decreasing trend of about -0.46 ppmv decade^{-1} in the tropical CPT SMRs. This cooling trend in the CPT implies that the observed increase of stratospheric water vapor is likely caused by changes in the residual circulation (Zhou et al. 2001; Zhou 2000).

Detailed information about how tropospheric air parcels enter the tropical lower stratosphere across the tropical CPT is not clear due to the shortage of enough direct observations of water vapor near the tropopause. The degree of saturation of air parcels at the tropical CPT may complicate the estimation of the entry value of water vapor (Vömel and Oltmans 1999). However, the entry value of water vapor mixing ratio across the tropical tropopause still depends on the longtime and large-scale mean, compared with convection, of the tropical tropopause temperatures (e.g., Mote et al. 1996). As long as the way in which the air enters the stratosphere has not changed, it is reasonable to expect low-frequency variations in the entry value of water vapor.

5. Summary

The principal points of this paper are as follows:

1) Our spline fitting method gives reasonable results for studying the morphology of the cold-point tropopause. However, ECMWF reanalyses systematically overestimate temperatures at the tropical CPT by 2–2.6 K. The warm bias in NCEP reanalyses is even larger.
2) The tropical western Pacific is the main part of the stratospheric fountain throughout the year. The region of concentration of daily minimum CPT SMR locations spreads in longitude throughout much of the year and is displaced northward during the time of the Indian summer monsoon.
3) There are three major variabilities in the tropical CPT. They are intraseasonal variability, the seasonal cycle, and low-frequency variabilities. Much of the low-frequency variabilities of the tropical CPT are closely related to the stratospheric QBO and the tropospheric ENSO.
4) The stratospheric QBO fingerprints in the tropical CPT are mainly zonally symmetric, while the ENSO fingerprints in the CPT have distinct E–W dipole and N–S dumbbell features. The ENSO fingerprints in the CPT are stronger than the QBO fingerprints in the CPT.
5) Both the ENSO and QBO fingerprints in the CPT temperatures are large enough to give significant variations in the tropical CPT SMR, and therefore

should affect the entry value of water vapor across the tropical CPT into the lower stratosphere.
6) ENSO and tropical CPT temperatures are simultaneously correlated while the stratospheric QBO in 50 mb wind shear is not simultaneously correlated.
7) The QBO signature in the tropical CPT is probably caused by the downward-propagating QBO meridional circulation in the equatorial stratosphere.
8) Tropical convection is suggested to explain much of the low-frequency variabilities of the tropical CPT. This is supported by observations and theoretical analysis (Yulaeva and Wallace 1994; Zhou and Sun 1994; Zhou et al. 2001).

Acknowledgments. This research was supported by NASA under SAGE Grant NAS 196006 to SUNY at Stony Brook. We thank Drs. Andrew Dessler and Paul Newman for providing us with the radiosonde data set that we used in this paper. We thank Dr. James Holton for leading us to Yulaeva and Wallace (1994). We also thank two anonymous reviewers for their helpful comments and suggestions. Preparation of the final version was supported in part by NASA Grant NAG-5-7090 to the University of Washington.

REFERENCES

Abbas, M. M., and Coauthors, 1996: Seasonal variations of the water vapor in the lower stratosphere inferred from ATMOS/ATLAS-3 measurements of H2O and CH4. *Geophys. Res. Lett.,* **23,** 2401–2404.

Andrews, D. G., J. R. Holton, and C. B. Leovy, 1987: *Middle Atmospheric dynamics.* International Geophysical Series, Vol. 40, Academic Press, 489 pp.

Angell, J. K., 1993: Comparison of stratospheric warming following Agung, El Chichon, and Pinatubo volcanic erutions. *Geophys. Res. Lett.,* **20,** 715–718.

Arkin, P. A., 1984: An examination of the Southern Oscillation in the upper tropospheric tropical and subtropical wind-field. Ph.D thesis, University of Maryland at College Park, MD, 240 pp.

Atticks, M., and G. Robinson, 1983: Some features of the structure of the tropical tropopause. *Quart. J. Roy. Meteor. Soc.,* **109,** 295–308.

Danielsen, E. F., 1993: *In situ* evidence of rapid, vertical, irreversible transport of lower tropospheric air into the lower tropical stratosphere by convective cloud turrets and by large-scale upwelling in tropical cyclones. *J. Geophys. Res.,* **98,** 8665–8681.

Dessler, A. E., 1998: A reexamination of the ''stratospheric fountain'' hypothesis. *Geophys. Res. Lett.,* **25,** 4165–4168.

——, E. M. Weinstock, E. J. Hinsta, J. G. Anderson, C. W. Webster, R. D. May, J. W. Elkins, and G. S. Dutton, 1994: An examination of the total hydrogen budget of the lower stratosphere. *Geophys. Res. Lett.,* **21,** 2563–2566.

Frederick, J. E., and A. R. Douglass, 1983: Atmospheric temperatures near the tropical tropopause: Temporal variations, zonal asymmetry and implications for stratospheric water vapor. *Mon. Wea. Rev.,* **111,** 1397–1401.

Gage, K. S., and G. Reid, 1987: Longitudinal variations in tropical tropopause properties in relation to tropical convection and ENSO events. *J. Geophys. Res.,* **92,** 14 197–14 203.

——, J. R. McAfee, D. A. Carter, W. L. Ecklund, A. C. Riddle, G. C. Reid, and B. B. Balsley, 1991: Long-term mean vertical motion over the tropical Pacific: Wind-profiling Doppler radar measurements. *Science,* **254,** 1771–1773.

Geller, M. A., W. Shen, M. Zhang, and W. Tan, 1997: Calculation of the stratospheric quasi-biennial oscillation for time-varying wave forcing. *J. Atmos. Sci.,* **54,** 883–894.

Gettelman, A., J. R. Holton, and A. R. Douglass, 2000: Simulations of water vapor in the lower stratosphere and upper troposphere. *J. Geophys. Res.,* **105,** 9003–9023.

Gibson, J. K., P. Kallberg, S. Uppala, A. Hernandez, A. Nomura, and E. Serrano, 1997: ERA description. ECMWF Reanalyses Project Report Series, No. 1, ECMWF, 71 pp.

Gill, A. E., 1980: Some simple solutions for heat-induced tropical circulation. *Quart. J. Roy. Meteor. Soc.,* **106,** 447–462.

Hamming, R. W., 1989: *Digital Filter.* Prentice-Hall. 3d ed. 284 pp.

Hanson, A. R., and G. D. Robinson, 1989: Water vapor and methane in the upper stratosphere: An examination of some of the Nimbus measurements. *J. Geophys. Res.,* **94,** 8474–8484.

Highwood, E. J., and B. J. Hoskins, 1998: The tropical tropopause. *Quart. J. Roy. Meteor. Soc.,* **124,** 1579–1604.

Holton, J. R., P. H. Haynes, M. E. McIntyre, A. R. Douglass, R. B. Rood, and L. Pfister, 1995: Stratosphere–troposphere exchange. *Rev. Geophys.,* **33,** 405–439.

Jones, R. L., P. P. Bhatt, and J. M. Russell III, 1986: The water vapor budget of the stratosphere studied using LIMS and the SAMS satellite data. *Quart. J. Roy. Meteor. Soc.,* **112,** 1127–1143.

Meehl, G. A., 1993: A coupled air–sea biennial mechanism in the tropical Indian and Pacific regions: Role of the ocean. *J. Climate,* **6,** 31–40.

Mote, P. W., and Coauthors, 1996: An atmospheric tape recorder: The imprint of tropical tropopause temperatures on stratospheric water vapor. *J. Geophys. Res.,* **101,** 3989–4006.

Naujokat, B., 1986: An update of the observed quasi-bieenial oscillation of the stratospheric winds over the Tropics. *J. Atmos. Sci.,* **43,** 1873–1877.

Newell, R. E., and S. Gould-Stewart, 1981: A stratospheric fountain. *J. Atmos. Sci.,* **38,** 2789–2795.

Oort, A. H., and J. J. Yienger, 1996: Observed interannual variability in the Hadley circulation and its connection to ENSO. *J. Climate* **9,** 2751–2767.

Pawson, S., and M. Fiorino, 1998: A comparison of reanalyses in the tropical stratosphere. Part 1: Thermal structure and the annual cycle. *Climate Dyn.,* **14,** 631–644.

Plumb, R. A., and R. C. Bell, 1982: A model of the quasi-biennial oscillation on an equatorial beta-plane. *Quart. J. Roy. Meteor. Soc.,* **108,** 335–352.

Randel, W. J., F. Wu, and D. J. Gaffen, 2000: Low frequency varirations of the tropical tropopause from NCEP reanalyses. *J. Geophys. Res.,* **105,** 15 509–15 523.

Reed, R. J., W. J. Campbell, L. A. Rasmussen, and D. G. Rogers, 1961: Evidence of downward-propagating annual wind reversal in the equatorial stratosphere. *J. Geophys. Res.,* **66,** 813–818.

Reid, G. C., 1994: Seasonal and interannual temperature variations in the tropical stratosphere. *J. Geophys. Res.,* **99,** 18 923–18 932.

——, and K. S. Gage, 1981: On the annual variation in height of the tropical tropopause. *J. Atmos. Sci.,* **38,** 1928–1938.

——, and ——, 1985: Interannual variation in the height of the tropical tropopause. *J. Geophys. Res.,* **90,** 5629–5635.

——, and ——, 1996: The tropical tropopause over the western Pacific: wave driving, convection, and the annual cycle. *J. Geophys. Res.,* **101,** 21 233–21 242.

Remsberg, E. E., P. P. Bhatt, and J. M. Russell III, 1996: Estimation of the water vapor budget of the stratosphere from UARS HALOE data. *J. Geophys. Res.,* **101,** 6749–6766.

Ropelewski, C. F., M. S. Halpert, and X. Wang, 1992: Observed tropospheric biennial variability and its relationship to the Southern Oscillation. *J. Climate,* **5,** 594–614.

Sherwood, S. C., 1999: A ''stratospheric drain'' over the marine continent. *Eos, Trans. Amer. Geophys. Union,* **80** (Suppl.), S62.

Teitelbaum, H., M. Moustaoui, C. Basdevant, and J. R. Holton, 2000: An alternative mechanism explaining the hygropause formation in tropical region. *Geophys. Res. Lett.,* **27,** 221–224.

Trenberth, K. E., 1997: The definition of El Niño. *Bull. Amer. Meteor. Soc.,* **78,** 2771–2777.
Veryard, R. G., and R. A. Ebdon, 1961: Fluctuations in tropical stratospheric winds. *Meteor. Mag.,* **90,** 125–143.
Vömel, H., and S. J. Oltmans, 1999: Comments on ''A reexamination of the 'stratospheric fountain' hypothesis by A. E. Dessler.'' *Geophys. Res. Lett.,* **26,** 2737–2738.
Waliser, D. E., and W. F. Zhou, 1997: Removing satellite equatorial crossing time biases from the OLR and HRC datasets. *J. Climate,* **10,** 2125–2146.
Xu, J. S., 1992: On the relationship between the stratospheric quasi-biennial oscillation and the tropospheric Southern Oscillation. *J. Atmos. Sci.,* **49,** 725–734.
Yulaeva, E., J. R. Holton, and J. M. Wallace, 1994: On the cause of annual cycle in the tropical lower stratospheric temperature. *J. Atmos. Sci.,* **51,** 169–174.
——, and J. M. Wallace, 1994: The signature of ENSO in global temperature and precipitation fields derived from the microwave sounding unit. *J. Climate,* **7,** 1719–1736.
Zhou, X. L., 2000: The tropical cold point tropopause and stratospheric water vapor. Ph.D. dissertation, State University of New York at Stony Brook, 121 pp.
——, and Z. Sun, 1994: Tropical atmospheric nonlinear steady response solution under effects of paired heat sources of contrasting nature. *ACTA Meteor. Sin.,* **8,** 356–364.
——, and M. A. Geller, 1998: Interannual variabilities of lower stratospheric water vapor. *Eos, Trans. Amer. Geophys. Union,* **79,** (Suppl.), S52.
——, ——, and M. H. Zhang, 2001: The cooling trend of the tropical cold point tropopause temperatures and its implications. *J. Geophys. Res.,* **106,** 1511–1522.